

See discussions, stats, and author profiles for this publication at: <https://www.researchgate.net/publication/314980253>

Strong Spin-Phonon Coupling Mediated by Single Ion Anisotropy in the All-In-All-Out Pyrochlore Magnet $\text{Cd}_2\text{Os}_2\text{O}_7$

Article in *Physical Review Letters* · March 2017

DOI: 10.1103/PhysRevLett.118.117201

CITATIONS

0

READS

13

11 authors, including:



Chang Hee Sohn

Seoul National University

22 PUBLICATIONS 92 CITATIONS

SEE PROFILE



Hien Thi Minh Nguyen

Seoul National University

21 PUBLICATIONS 137 CITATIONS

SEE PROFILE



Kyungwan Kim

Chungbuk National University

54 PUBLICATIONS 1,430 CITATIONS

SEE PROFILE

Strong Spin-Phonon Coupling Mediated by Single Ion Anisotropy in the All-In–All-Out Pyrochlore Magnet $\text{Cd}_2\text{Os}_2\text{O}_7$

C. H. Sohn,^{1,2} C. H. Kim,^{1,2} L. J. Sandilands,^{1,2} N. T. M. Hien,^{1,2} S. Y. Kim,^{1,2} H. J. Park,^{1,2} K. W. Kim,³ S. J. Moon,⁴ J. Yamaura,⁵ Z. Hiroi,⁶ and T. W. Noh^{1,2}

¹Center for Correlated Electron Systems, Institute for Basic Science (IBS), Seoul 151-742, Republic of Korea

²Department of Physics and Astronomy, Seoul National University, Seoul 151-742, Republic of Korea

³Department of Physics, Chungbuk National University, Cheongju, Chungbuk 28644, Republic of Korea

⁴Department of Physics, Hanyang University, Seoul 133-791, Republic of Korea

⁵Materials Research Center for Element Strategy, Tokyo Institute of Technology, Kanagawa 226-8503, Japan

⁶ISSP, University of Tokyo, Kashiwa 277-8581, Japan

(Received 22 August 2016; revised manuscript received 22 January 2017; published 13 March 2017)

Spin-phonon coupling mediated by single ion anisotropy was investigated using optical spectroscopy and first-principles calculations in the all-in–all-out pyrochlore magnet $\text{Cd}_2\text{Os}_2\text{O}_7$. Clear anomalies were observed in both the phonon frequencies and linewidths at the magnetic ordering temperature. The renormalization of the phonon modes was exceptionally large, signifying the presence of an unconventional magnetoelastic term from large spin-orbit coupling. In addition, the relative phonon frequency shifts show a strong correlation with the modulation of noncubic crystal field by the corresponding lattice distortion. Our observation establishes a new type of spin-phonon coupling through single ion anisotropy, a second-order spin-orbit coupling term, in $\text{Cd}_2\text{Os}_2\text{O}_7$.

DOI: 10.1103/PhysRevLett.118.117201

Novel spin-lattice coupling via the spin-orbit (SO) interaction is essential for stabilizing peculiar magnetic ordering in $5d$ transition metal oxides (TMOs). The collective ordering of spins on a periodic lattice and their mutual interaction have long been a central theme in condensed matter physics. Most of these phenomena could be understood by considering the exchange interactions between spins. However, recent studies on $5d$ TMOs have revealed the critical role SO coupling plays in their magnetism. Since the orbitals are generically coupled to the lattice, the large SO coupling present in $5d$ orbitals creates strong and inevitable interactions between spin and lattice, causing the spin to reflect characteristics of the lattice and thereby stabilize peculiar magnetic order. In Sr_2IrO_4 , for instance, the spins follow the rotation of the octahedra via the Dzyaloshinskii-Moriya (DM) interaction [1,2]. Particularly, such spin-lattice coupling can be more important in the frustrated lattices, i.e., pyrochlore iridates and osmates [3–8], where long-range ordering is stabilized by SO-mediated interactions [9–12]. Although intensive studies have been performed to investigate the unusual magnetism in $5d$ TMOs, a detailed understanding of spin-lattice coupling mediated by SO interaction has not yet been achieved.

The $5d$ pyrochlore $\text{Cd}_2\text{Os}_2\text{O}_7$ represents an excellent material in which to study unconventional spin-lattice coupling. In this compound, the superexchange (SE) interaction between magnetic Os spins is highly frustrated as the spins are arranged on tetrahedra. On the other hand, large single ion anisotropy (SIA), a second-order SO coupling effect, induces the Os spins to align preferentially

along the local trigonal distortion axes [11,12]. This preference stabilizes the peculiar all-in–all-out (AIAO) magnetic ordering, where all spins point inward in one tetrahedron and outward in the adjacent one, below $T_N = 227$ K [6,7]. $\text{Cd}_2\text{Os}_2\text{O}_7$ therefore represents an opportunity to study unconventional magnetoelastic effects mediated by SO coupling beyond the conventional mechanism based on the modulation of SE interactions.

Here, we demonstrate using optical spectroscopy and first-principles calculations that SIA leads to strong spin-phonon coupling in $\text{Cd}_2\text{Os}_2\text{O}_7$. We observed clear anomalies in the frequencies and linewidths of the infrared (IR) phonon modes at T_N , indicating a strong coupling between lattice dynamics and the AIAO magnetic phase transition. The broadening and frequency shift is exceptionally large, implying an enhanced magnetoelastic coupling due to the SO interaction. Based on the phonon eigenmodes from first-principles calculation, we found a strong correlation between the relative phonon frequency shift and crystal electric field (CEF) modulation by the corresponding phonon modes. Our finding establishes a new type of spin-phonon coupling mechanism through SIA.

Temperature (T)-dependent optical spectroscopy and first-principles calculations were used to investigate the evolution of IR-active phonon spectra through T_N in $\text{Cd}_2\text{Os}_2\text{O}_7$. The real part of the optical conductivity, $\sigma_1(\omega)$, was obtained from near-normal reflectance and ellipsometry measurements [13]. The first-principles calculations were performed using density functional theory + U with the PBEsol exchange correlation functional implemented in VASP [14].

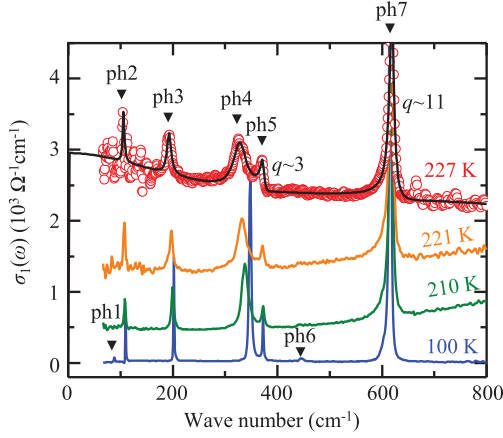


FIG. 1. T -dependent $\sigma_1(\omega)$ below 800 cm^{-1} . Seven phonon modes are highlighted by solid triangles. The black solid line indicates the best fitting results for the 227 K data with Lorentz and Fano oscillators. The asymmetry parameter q for the two asymmetric modes are indicated.

The frozen phonon method was used to calculate the zone-center phonons, and $U_{\text{eff}} = 1.5 \text{ eV}$ was chosen to simulate the local Hubbard interaction in Os. AIAO magnetic ordering was considered within a noncollinear density functional theory formalism.

In Fig. 1, $\sigma_1(\omega)$ shows the T -dependent IR phonon modes of $\text{Cd}_2\text{Os}_2\text{O}_7$. The increase in intensity of the broad background with T corresponds to the emergence of free carriers via the Lifshitz metal-insulator transition [13]. The sharp peaks marked by triangles (from ph1 to ph7) correspond to the seven IR phonon modes expected for the pyrochlore structure [15]. Among them, ph1 and ph6 are visible only at low T due to their weak intensity while the other five phonons are clearly seen at high T . ph5 and ph7 show an asymmetric Fano line shape [16] at high T , indicating considerable electron-phonon interaction. ph2, ph3, and ph4, on the other hand, remain symmetric. All phonon modes show a sizable T dependence of the linewidth and frequencies.

To quantify the T evolution of the phonon modes, we fitted $\sigma_1(\omega)$ using a minimal model. Drude and CPM_0 models were utilized to fit the broad electronic background [13]. Because the intensities of ph1 and ph6 are too weak, these modes were not analyzed. We used two Fano oscillators for the asymmetric ph5 and ph7 modes and three Lorentz oscillators for the ph2, ph3, and ph4 modes. The black solid line in Fig. 1 is the best fitting result for the 227 K data. The T -dependent phonon frequency [$\omega(T)$], the linewidth [$\Gamma(T)$], and the phonon plasma frequency [$\Omega(T)$] were obtained from the fitting for each phonon

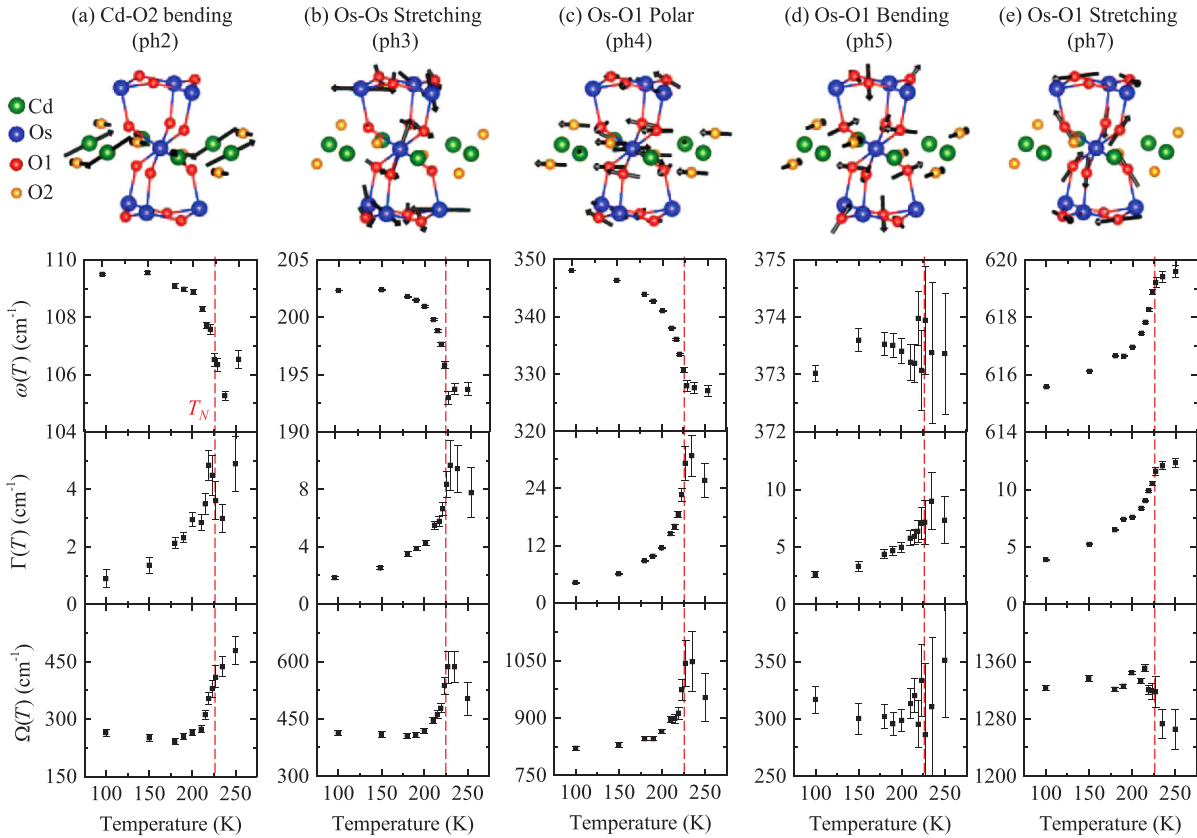


FIG. 2. Eigenvectors, $\omega(T)$, $\Gamma(T)$, and $\Omega(T)$ of the (a) Cd-O2 bending, (b) Os-Os stretching, (c) Os-O1 polar, (d) Os-O1 bending, and (e) Os-O1 stretching modes. The black solid arrows in the top panels indicate the displacement of the ions by each phonon mode. The red dashed lines indicate T_N .

TABLE I. Phonon frequencies (cm^{-1}) from $\sigma_1(\omega)$ at 100 K, from first-principles calculations, and eigenmodes from first-principles calculations.

	$\sigma_1(\omega)$	DFT	Eigenmode	Remark
ph1	88.7	84.6	Cd-OsO ₆ stretching	Weak intensity
ph2	109.5	107.1	Cd-O2 bending	...
ph3	202.3	200.2	Os-Os stretching	...
ph4	348.0	367.4	Os-O1 polar	...
ph5	373.0	363.9	Os-O1 bending	Asymmetric
ph6	445.5	444.4	Cd-O2 stretching	Weak intensity
ph7	615.6	618.5	Os-O1 stretching	Asymmetric

mode, as shown in Fig. 2. All phonon parameters show a clear kink at T_N , indicating that the lattice dynamics of $\text{Cd}_2\text{Os}_2\text{O}_7$ are strongly coupled to the AIAO magnetic phase transition.

For further understanding of the phonon renormalization, first-principles calculations were used to assign the observed phonon modes. Table I shows the phonon frequencies from the experimental $\sigma_1(\omega)$ at 100 K and from the calculations. Experimental and theoretical values show good agreement. By analyzing the main modulation of ions in the calculated eigenmodes, the seven modes were denoted as Cd-OsO₆ stretching, Cd-O2 bending, Os-Os stretching, Os-O1 polar, Os-O1 bending, Cd-O2 stretching, and Os-O1 stretching modes in the order of increasing phonon energies. The displacements of the ions near one Os ion in the five phonon modes are shown in the top panels of Fig. 2(a)–2(e). Here, O1 and O2 indicate oxygen that does and does not form OsO₆ octahedra, respectively. For the Os-O1 polar and bending modes, it is difficult to distinguish the two modes by frequency alone because they are close to each other. As the calculated intensities (dipole moment) of the Os-O1 polar mode is much larger than that of the Os-O1 bending mode, we assigned the ph4 (ph5) phonon to the Os-O1 polar (bending) mode. This assignment is also consistent with the fact that the Fano asymmetry exist only in ph5 and ph7; Os-O1 bending and stretching modes modulate the electron hopping path significantly and so should strongly couple to the electronic background.

In general, we can write down the phonon self-energy Σ as follows:

$$\Sigma = \Sigma_{\text{pp}} + \Sigma_{\text{ep}} + \Sigma_{\text{sp}}, \quad (1)$$

where Σ_{pp} , Σ_{ep} , and Σ_{sp} are the self-energies from phonon-phonon, electron-phonon, and spin-phonon interactions, respectively. Σ_{pp} is a smooth function of T and cannot explain the anomalies at T_N . Note that $\text{Re}[\Sigma_{\text{ep}}]$ is generally negative [17–19], while $\text{Re}[\Sigma_{\text{sp}}]$ can be positive or negative depending on the detailed magnetic Hamiltonian and phonon modes. In $\text{Cd}_2\text{Os}_2\text{O}_7$, the metal-insulator transition is accompanied by magnetic ordering; thus, both Σ_{ep} and

Σ_{sp} could, in principle, be the origin of the observed anomalies at T_N .

There are at least four reasons why Σ_{sp} is the dominant effect, rather than Σ_{ep} . First, the absence of a Fano line shape in ph2, ph3, and ph4 indicates weak electron-phonon coupling in these modes [16]. Second, if the phonons are well screened by free electrons, then Ω should decrease with the increasing number of free carriers at high T [20]. The increase in Ω in ph2, ph3, and ph4 in Figs. 2(a)–2(c) indicates a poor electron screening effect. Third, as $\text{Re}[\Sigma_{\text{ep}}]$ is always negative, Σ_{ep} cannot explain the softening of ph5 and ph7 with decreasing T . One plausible explanation is that Σ_{sp} softens ph5 and ph7 to a larger magnitude than Σ_{ep} even in the asymmetric ph5 and ph7. Finally, the linewidth broadening is also inconsistent with Σ_{ep} . The linewidth broadening by Σ_{ep} is proportional to a matrix element of the electron-phonon interaction [19]. Given their asymmetric line shapes, we would expect this effect to be most pronounced in ph5 and ph7. However, the linewidth broadening of ph5 and ph7 is in fact smaller than in the more symmetric ph2, ph3, and ph5 modes. This implies that Σ_{sp} , not Σ_{ep} , is the main contributor to the phonon anomalies at T_N .

The renormalization of the optical phonons at T_N in $\text{Cd}_2\text{Os}_2\text{O}_7$ is unusually large, implying the presence of peculiar magnetoelastic coupling mediated by SO coupling. Figure 3(a) shows $\Delta\omega/\omega_0$ and $\Delta\Gamma/\omega_0$ of five phonon modes, where ω_0 is the frequency at 100 K and $\Delta\omega$ and $\Delta\Gamma$ are the differences between the 100 and 227 K data. Both

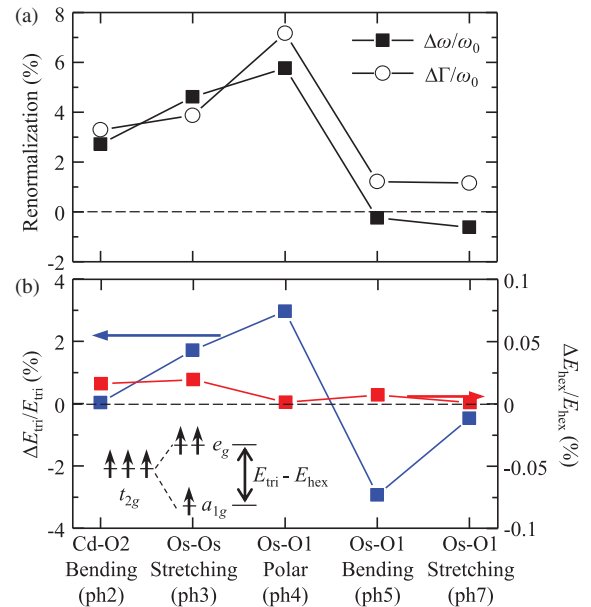


FIG. 3. (a) $\Delta\omega/\omega_0$ (solid squares) and $\Delta\Gamma/\omega_0$ (open circles) of five phonon modes. (b) Normalized trigonal and hexagonal crystal field change with the corresponding lattice distortion. The inset shows a schematic diagram of the orbital states of the Os ions.

linewidth broadening and frequency shift in ph_4 , for example, are over 5%. These values are unusually large, in that $\Delta\omega/\omega_0$ and $\Delta\Gamma/\omega_0$ are generally 1% or less in many 3d and 4d TMOs [21–25], where spin-phonon coupling mainly originates from the modulation of SE interactions. Similarly large renormalizations have been reported only in special cases where unconventional spin-phonon coupling mechanisms were proposed [26–29]. The most plausible mechanism here is the strong SO coupling in 5d systems, because the orbital contribution to the magnetism by SO coupling can lead to an *enhanced* magnetoelastic coupling.

The known magnetic Hamiltonian shows that a SO-mediated magnetoelastic coupling term should emerge from the modulation of SIA [12]. The Hamiltonian is

$$H = J \sum_{\langle i,j \rangle} \vec{S}_i \cdot \vec{S}_j + D \sum_i (\vec{S}_i \cdot \vec{A}_i)^2 + d \sum_{\langle i,j \rangle} \vec{e}_{ij} \cdot [\vec{S}_i \times \vec{S}_j], \quad (2)$$

where the first, second, and third terms correspond to the SE, SIA, and the DM term, respectively. According to quantum chemistry calculations and x-ray scattering measurements, the values of J , D , and d are about 6.4, -6.8 , and 1.7 meV, respectively [12,30]. Ignoring the small DM term, we can express the renormalization of the frequency as

$$\Delta\omega \sim \frac{1}{2\mu\omega} \left(\sum_{\langle i,j \rangle} \frac{\partial^2 J_{ij}}{\partial \vec{u}^2} \langle \vec{S}_i \cdot \vec{S}_j \rangle + \sum_i \frac{\partial^2 D_i}{\partial \vec{u}^2} \langle (\vec{S}_i \cdot \vec{A}_i)^2 \rangle \right), \quad (3)$$

where \vec{u} and μ are the atomic displacement and reduced mass of phonon modes, respectively [21]. Beyond the first SE term, the additional second term emerges from the modulation of SIA. We expect that the second term should govern the phonon renormalization here, because (i) it is an orbital contribution which generically couples to the lattice and (ii) the first SE term is expected to be suppressed in $\text{Cd}_2\text{Os}_2\text{O}_7$ as we will discuss later.

A simple CEF calculation was employed to elucidate the spin-phonon coupling via SIA. The microscopic origin of SIA is noncubic CEF in the presence of SO coupling [12]: noncubic CEF cause orbital anisotropy which is then transferred to the spin degree of freedom via SO coupling. According to a previous quantum chemistry calculation [12], the SIA in $\text{Cd}_2\text{Os}_2\text{O}_7$ is mainly caused by trigonal crystal fields (E_{tri}) due to the O ions and hexagonal crystal fields (E_{hex}) due to the Cd ions. Therefore, if the spin-phonon coupling is mostly caused by SIA, there should be a strong correlation between the size of the renormalization at T_N and the change in CEF energy associated with a given phonon modes.

To calculate the CEF change due to each phonon, we displaced each atom about the order of 0.01 Å along a

direction determined by the DFT eigenmode. Then, we used hydrogenlike atomic d wave functions with effective nuclear charge $Z = 8$ to describe the Os wave functions and a point charge model for the O and Cd ions. First-order perturbation theory in the a_{1g} and e_g orbital basis was then employed to calculate the modulation of E_{tri} (ΔE_{tri}) and E_{hex} (ΔE_{hex}) in the distorted structures. Figure 3(b) shows the calculated $\Delta E_{\text{tri}}/E_{\text{tri}}$ and $\Delta E_{\text{hex}}/E_{\text{hex}}$ by each phonon mode. A positive (negative) value indicates that the energy difference between the a_{1g} and e_g orbitals is decreased (increased) by the phonon mode. Since D is roughly proportional to the $a_{1g} - e_g$ splitting with a negative sign [12], positive (negative) changes induce a hardening (softening) of phonon mode below T_N [see the Eq. (3)].

Indeed, this calculation mostly explain the direction and relative magnitude of the phonon renormalization. The Os-Os stretching and Os-O1 polar modes are seen to strongly increase the trigonal CEF, consistent with the fact that these modes show strong hardening behavior. For the Os-O1 bending and stretching modes, $\Delta E_{\text{tri}}/E_{\text{tri}}$ is negative, which explains the softening of these two modes in experiment. Note that the magnitude of $\Delta E_{\text{tri}}/E_{\text{tri}}$ in the Os-O1 bending mode is quite large in contrast to weak energy shift in experiment. Since this mode show the most anisotropic Fano line shape, the discrepancy between the calculation and the experiments can be understood in terms of the competition between spin-phonon and electron-phonon coupling discussed above. Compared to $\Delta E_{\text{tri}}/E_{\text{tri}}$, $\Delta E_{\text{hex}}/E_{\text{hex}}$ is orders of magnitude smaller so it is unlikely to be the main contributor to the phonon renormalization. However, the small $\Delta E_{\text{hex}}/E_{\text{hex}}$ could be important for the Cd-O2 bending mode because of the small phonon energy and the absence of other possible interactions. $\Delta E_{\text{hex}}/E_{\text{hex}}$ by this phonon shows a small positive values, consistent with the hardening seen in Fig. 2(a). Overall, our crystal field calculation clearly show that the phonon renormalization at T_N in $\text{Cd}_2\text{Os}_2\text{O}_7$ mainly originates from the unconventional, SIA-mediated mechanism.

Before finishing, we want to briefly discuss the reduced effect of the SE term [first part of Eq. (3)] on the phonon renormalization in this compound. There are twelve non-equivalent Os-O1-Os bonds in the pyrochlore unit cell and the SE interactions are sensitive to their angles and lengths. We found that, although a given mode can modulate each angle and length significantly, it barely alters the average values. As a result, the SE terms are canceled out to first order. For a quantitative comparison, we calculated the modulation of the SE interaction with the distorted structure we used above for the Os-O1 bending mode, because this mode strongly modulates the SE interaction. We adopted an empirical expression for the SE interaction, $J(\phi) = J_{90} \sin^2[\phi] + J_{180} \cos^2[\phi]$, where J_{90} , J_{180} , and ϕ are J for 90, 180 degrees, and bond angle, respectively [31]. Using the known structure and J of NaOsO_3 [32] and $\text{Cd}_2\text{Os}_2\text{O}_7$, we estimated J_{90} and J_{180} as

–7.29 and 18.7 meV, respectively. $\Delta J/J$ with the distorted structure is only about 0.3%, 1 order of magnitude smaller than the trigonal crystal field terms. This further supports our claim that the SIA term governs spin-phonon coupling in $\text{Cd}_2\text{Os}_2\text{O}_7$.

In summary, a new type of spin-phonon coupling in $\text{Cd}_2\text{Os}_2\text{O}_7$ was investigated by optical spectroscopy and first-principles calculations. We observed large renormalizations of the phonon modes below T_N and a strong correlation between the phonon shift and the CEF modulation, which consistently supports spin-phonon coupling through SIA, one of the SO coupling terms. We emphasize that the observed spin-phonon coupling mediated by SO coupling is not specific to $\text{Cd}_2\text{Os}_2\text{O}_7$, but is a characteristic feature of $5d$ TMOs. Beyond SE interactions, spin, orbital, and lattice degrees of freedom in $5d$ TMOs should be strongly coupled to each other via various SO-mediated interactions, such as DM, SIA, and pseudodipolar interactions. Our results motivate further systematic studies including high magnetic field or pressure experiments on $5d$ layered perovskite, honeycomb, and pyrochlore compounds.

This work was supported by the Research Center Program of IBS (Institute for Basic Science) in Korea (IBS-R009-D1). S.J.M. and K.W.K. were supported by Basic Science Research Program through the National Research Foundation of Korea (NRF) funded by the Ministry of Science, ICT and Future Planning (NRF-2014R1A2A1A11054351 and NRF-2015R1A2A1A10056200, respectively).

-
- [1] B. J. Kim, H. Jin, S. J. Moon, J.-Y. Kim, B.-G. Park, C. S. Leem, J. Yu, T. W. Noh, C. Kim, S.-J. Oh, J.-H. Park, V. Durairaj, G. Cao, and E. Rotenberg, *Phys. Rev. Lett.* **101**, 076402 (2008).
- [2] B. J. Kim, H. Ohsumi, T. Komesu, S. Sakai, T. Morita, H. Takagi, and T. Arima, *Science* **323**, 1329 (2009).
- [3] S. Zhao, J. M. Mackie, D. E. MacLaughlin, O. O. Bernal, J. J. Ishikawa, Y. Ohta, and S. Nakatsuji, *Phys. Rev. B* **83**, 180402(R) (2011).
- [4] K. Tomiyasu, K. Matsuhira, K. Iwasa, M. Watahiki, S. Takagi, M. Wakeshima, Y. Hinatsu, M. Yokoyama, K. Ohoyama, and K. Yamada, *J. Phys. Soc. Jpn.* **81**, 034709 (2012).
- [5] H. Sagayama, D. Uematsu, T. Arima, K. Sugimoto, J. J. Ishikawa, E. O'Farrell, and S. Nakatsuji, *Phys. Rev. B* **87**, 100403(R) (2013).
- [6] D. Mandrus, J. R. Thompson, R. Gaal, L. Forro, J. C. Bryan, B. C. Chakoumakos, L. M. Woods, B. C. Sales, R. S. Fishman, and V. Keppens, *Phys. Rev. B* **63**, 195104 (2001).
- [7] J. Yamaura, K. Ohgushi, H. Ohsumi, T. Hasegawa, I. Yamauchi, K. Sugimoto, S. Takeshita, A. Tokuda, M. Takata, M. Udagawa, M. Takigawa, H. Harima, T. H. Arima, and Z. Hiroi, *Phys. Rev. Lett.* **108**, 247205 (2012).
- [8] S. Tardif, S. Takeshita, H. Ohsumi, J. I. Yamaura, D. Okuyama, Z. Hiroi, M. Takata, and T. H. Arima, *Phys. Rev. Lett.* **114**, 147205 (2015).
- [9] T.-h. Arima, *J. Phys. Soc. Jpn.* **82**, 013705 (2013).
- [10] M. Elhajal, B. Canals, R. Sunyer, and C. Lacroix, *Phys. Rev. B* **71**, 094420 (2005).
- [11] H. Shinaoka, T. Miyake, and S. Ishibashi, *Phys. Rev. Lett.* **108**, 247204 (2012).
- [12] N. A. Bogdanov, R. Maurice, I. Rousochatzakis, J. van den Brink, and L. Hozoi, *Phys. Rev. Lett.* **110**, 127206 (2013).
- [13] C. H. Sohn, H. Jeong, H. Jin, S. Kim, L. J. Sandilands, H. J. Park, K. W. Kim, S. J. Moon, D.-Y. Cho, J. Yamaura, Z. Hiroi, and T. W. Noh, *Phys. Rev. Lett.* **115**, 266402 (2015).
- [14] G. Kresse and J. Hafner, *Phys. Rev. B* **47**, 558 (1993).
- [15] N. T. Vandenborre, E. Husson, and H. Brusset, *Spectrochim. Acta, Part A* **37**, 113 (1981).
- [16] U. Fano, *Phys. Rev.* **124**, 1866 (1961).
- [17] M. Reizer, *Phys. Rev. B* **61**, 40 (2000).
- [18] C. O. Rodriguez, A. I. Liechtenstein, I. I. Mazin, O. Jepsen, O. K. Andersen, and M. Methfessel, *Phys. Rev. B* **42**, 2692 (1990).
- [19] D. Olego and M. Cardona, *Phys. Rev. B* **23**, 6592 (1981).
- [20] A. Akrap, J. J. Tu, L. J. Li, G. H. Cao, Z. A. Xu, and C. C. Homes, *Phys. Rev. B* **80**, 180502(R) (2009).
- [21] E. Granado, A. Garcia, J. A. Sanjurjo, C. Rettori, I. Torriani, F. Prado, R. Sanchez, A. Caneiro, and S. B. Oseroff, *Phys. Rev. B* **60**, 11879 (1999).
- [22] M. A. Quijada, J. R. Simpson, L. Vasiliu-Doloc, J. W. Lynn, H. D. Drew, Y. M. Mukovskii, and S. G. Karabashev, *Phys. Rev. B* **64**, 224426 (2001).
- [23] J. S. Lee, T. W. Noh, J. S. Bae, I.-S. Yang, T. Takeda, and R. Kanno, *Phys. Rev. B* **69**, 214428 (2004).
- [24] J. Laverdiere, S. Jandl, A. A. Mukhin, V. Y. Ivanov, V. G. Ivanov, and M. N. Iliev, *Phys. Rev. B* **74**, 179902(E) (2006).
- [25] Ch. Kant, J. Deisenhofer, T. Rudolf, F. Mayr, F. Schrettle, A. Loidl, V. Gnezdilov, D. Wulferding, P. Lemmens, and V. Tsurkan, *Phys. Rev. B* **80**, 214417 (2009).
- [26] S. Calder, J. H. Lee, M. B. Stone, M. D. Lumsden, J. C. Lang, M. Feyngenson, Z. Zhao, J.-Q. Yan, Y. G. Shi, Y. S. Sun, Y. Tsujimoto, K. Yamaura, and A. D. Christianson, *Nat. Commun.* **6**, 8916 (2015).
- [27] C. Ulrich, G. Khaliullin, M. Guennou, H. Roth, T. Lorenz, and B. Keimer, *Phys. Rev. Lett.* **115**, 156403 (2015).
- [28] H. Sakai, J. Fujioka, T. Fukuda, D. Okuyama, D. Hashizume, F. Kagawa, H. Nakao, Y. Murakami, T. Arima, A. Q. R. Baron, Y. Taguchi, and Y. Tokura, *Phys. Rev. Lett.* **107**, 137601 (2011).
- [29] A. F. Garcia-Flores, A. F. L. Moreira, U. F. Kaneko, F. M. Ardito, H. Terashita, M. T. D. Orlando, J. Gopalakrishnan, K. Ramesha, and E. Granado, *Phys. Rev. Lett.* **108**, 177202 (2012).
- [30] S. Calder, J. G. Vale, N. A. Bogdanov, X. Liu, C. Donnerer, M. H. Upton, D. Casa, A. H. Said, M. D. Lumsden, Z. Zhao, J.-Q. Yan, D. Mandrus, S. Nishimoto, J. van den Brink, J. P. Hill, D. F. McMorrow, and A. D. Christianson, *Nat. Commun.* **7**, 11651 (2016).
- [31] K. Motida and S. Miyahara, *J. Phys. Soc. Jpn.* **28**, 1188 (1970).
- [32] S. Calder, J. G. Vale, N. Bogdanov, C. Donnerer, M. Moretti Sala, X. Liu, M. H. Upton, D. Casa, Y. G. Shi, Y. Tsujimoto, K. Yamaura, J. P. Hill, J. van den Brink, D. F. McMorrow, and A. D. Christianson, *Phys. Rev. B* **95**, 020413 (2017).